STRESS INTENSITY FACTOR CALCULATIONS FOR CRACKS EMANATING FROM BOLT HOLES IN A JET ENGINE COMPRESSOR DISC

W. Beres, A.K. Koul
[1]*Institute for Aerospace Research, National Research Council Canada, Ottawa, Canada*
wieslaw.beres@nrc.ca
[2]*Life Prediction Technologies,Inc., Ottawa, Ontario, Canada*
koula@lifepredictiontech.com
Keywords: *gas turbine engine, life prediction, damage tolerance, stress intensity factor*

Abstract

This paper presents the results of finite element based stress and fracture mechanics analyses carried out on the compressor disc of a jet engine using two and three dimensional models. A total of ninety finite element models of the compressor disc were prepared, out of which 81 were two dimensional models and 9 were three dimensional. All models were prepared and analysed for the uncracked discs, discs with various numbers of cracks emanating from neighbouring bolt holes as well as for a disc with two cracks emanating from the same bolt hole. It was established that the primary fracture critical location in the compressor disc was the bolt hole surface closest to the disc centre and the secondary fracture critical location was the bolt hole surface closest to the disc rim.

Plastic zone size measurements ahead of tips in service-induced cracks were carried out using a microhardness technique and these values were used to estimate the stress intensity factors as a function of crack size. Quantitative fractography results were also used to estimate the stress intensity factors. There was a good agreement between numerical calculations and experimental data.

1 Introduction

Damage tolerance concepts for gas turbine engines have emerged due to the limitations of the traditional safe life design concept, where only 1 in 1000 components is expected to develop a 0.8 mm long crack at retirement. The rest of the 999 components are retired in a crack free condition and much of the useful life of rotating components such as discs and spacers is not utilized. In order to implement damage tolerance concepts in the field it is proposed to utilize the remaining usable life of each component by repeatedly inspecting the component after a predetermined safe inspection interval (SII) during which any undetected crack will not grow beyond the dysfunction crack size, and to retire the components on an individual basis, once a crack is detected.

In such a damage tolerance based maintenance methodology, it is assumed that flaws exist in parts as manufactured and that they are located in the fracture critical locations of the components. It is further assumed that these flaws will grow in service at a rate governed by the local stress distribution and operating environment for the parts. The primary objective of this fracture mechanics based approach is to compute a cyclic life versus crack length curve for a specific part up to a predetermined dysfunction crack size. This in turn is used to determine the safe inspection interval for implementation in the field. Also, appropriate NDI procedures are needed at the depot level to ensure that crack sizes much smaller than the dysfunction crack size are reliably detected to avoid the risk of catastrophic failure.

A number of analytical procedures have been proposed for computing safe inspection

intervals for aero engine discs and spacers. These include deterministic fracture mechanics approaches, probabilistic fracture mechanics approaches and their combinations, as described in [1],[2],[3],[4]. Damage tolerance analysis of any aerospace structural component involves the identification of the fracture critical location, determination of stress intensity factors (SIF) as a function of crack length and assessment of critical and dysfunction crack sizes. This assessment is usually carried out using approximate numerical methods, such as finite element (FE), finite difference or boundary element techniques. The accuracy of SIF calculation plays a major role on the accuracy and reliability of safe inspection interval predictions.

This paper presents the results of FE based stress and fracture mechanics analyses carried out on the compressor disc of a jet engine using two and three dimensional models. The FE based analytical results, in terms of stress intensity factors, are compared using results obtained on the basis of metallurgical analysis. The results obtained formed the basis for performing damage tolerance analysis for the compressor disc [3],[4].

2 Materials and calculation methods

2.1 The compressor disc of the jet engine

A front view of the compressor disc under investigation is presented in Fig. 1. Each disc contains forty bolt holes. In addition to the bolt holes, there are also 131 equidistant blade dovetail slots distributed on the disc circumference.

2.2 Disc material mechanical properties

The compressor disc is made from AM355, a precipitation-hardened martensitic stainless steel. All mechanical properties data for this steel that were used for performing finite element stress and fracture mechanics calculations were taken from reference [5].

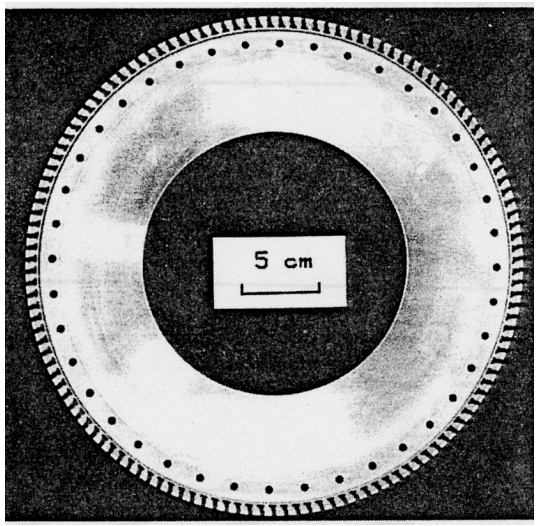

Fig. 1 A front view of the compressor disc

2.3 Disc loading

A rotating compressor disc is subjected to a combination of centrifugal, thermal and surface loads. Only centrifugal loads for the components were taken into account. Thermal stresses as well as surface loads were neglected in the calculations, because the radial temperature gradient was not very high.

2.3.1 Centrifugal loads due to the disc mass

The centrifugal load arising from the disc mass was determined through finite element calculations after defining the axis of disc rotation and using the disc material density and the maximum allowable disc rotational speed.

2.3.2 Centrifugal loads due to the blade mass

The centrifugal forces originating from the blades were calculated by applying pressure forces that were uniformly distributed along the middle radius of the blade attachment slots. These pressure forces were calculated by considering the mass of a single blade, the distance from the disc rotational axis to the centre of gravity of the blade and the rotational speed of the disc-blade assembly.

2.4 Finite element models for the compressor disc

The finite elements used for 2D calculations were: eight-node quadrilateral elements, six-node triangular elements and six-node singular triangular elements with mid-nodes shifted to quarter point positions, to model the stress field singularity around the crack tip. All elements were second-order, plane-stress elements with two degrees of freedom per node.

The thickness of particular plane stress finite elements was varied according to the local thickness of the disc region. A total of five different element thickness values were used along the disc radius to model the disc from the bore to the rim.

The finite elements used for 3D modelling were: twenty-node hexahedron elements, fifteen-node wedge elements, and fifteen-node singularity wedge elements with mid-nodes shifted to quarter point positions.

To simplify the calculations, only segments of the disc were modelled. The side lines of the two dimensional disc segment models and the side surfaces of the three dimensional models were assumed to slide and remain straight and flat.

Initially the calculations were performed on relatively simple 2D finite element models which were uncracked or contained one crack only. A total of ninety finite element models of the disc segment were prepared, out of which 81 were two-dimensional models and 9 were three dimensional models.

Twenty two models contained thru-thickness cracks of lengths that varied between 0.64 and 16 mm. In all cases the cracks emanated from the bolt hole surface in the direction of the disc bore, *i.e.* propagating radially inward. Four separate models containing cracks of lengths ranging between 0.64 and 4.2 mm, but emanating from the bolt hole surface in the direction of the disc rim, *i.e.* propagating radially outward, were also considered.

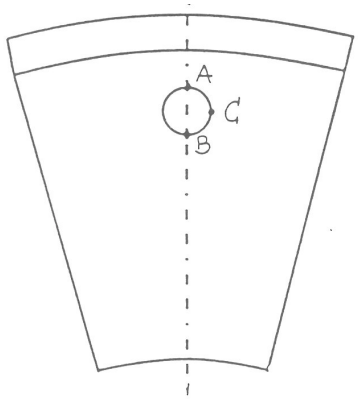

Fig. 2 Notation for different locations in a bolt hole

FE calculations were performed for the following crack configurations (Fig. 2):

- radially inward, single thru-thickness crack, emanating from point B in the bolt hole,
- radially outward, single thru-thickness crack, emanating from point A in the bolt hole,
- two thru-thickness cracks in one bolt hole, emanating from points A and B,
- two radially inward thru-thickness cracks of equal length emanating from point B in two neighbouring bolt holes,
- two radially inward thru-thickness cracks of equal length emanating from point B in two bolt holes separated by one uncracked bolt hole,
- radially inward thru-thickness cracks of equal length emanating from point B in each bolt hole,
- radially inward thru-thickness cracks of equal length emanating from point B in every second bolt hole,
- radially inward corner and surface cracks emanating from bolt holes at point B and lying in the plane parallel to the main disc rotation axis.

SIFs were extracted from each finite element calculation. Also, von Mises stresses were recovered for points A and B on the bolt hole circumference located directly opposite to the inward and outward cracks respectively.

To provide examples of typical finite element meshes used for 2D calculations, Fig. 3 presents the mesh for a disc segment with a sector angle of 27.0° containing a radially

inward crack of 16 mm in length. Eight six-node singular triangular finite elements with mid-nodes shifted to a quarter point position were located around the crack tip. This layout of elements around the crack tip was typical for all finite element models used for fracture mechanics analyses. This model, after modification, was also used for performing calculations on uncracked discs.

To provide an example of a typical finite element mesh used for 3D calculations, Fig. 4 shows the geometry of a model where a corner crack of 0.30 mm in radius, emanates from the bolt hole. Thirty two wedge elements with mid-nodes shifted to a quarter point position forming a circular crack front were used. This layout of elements around the crack front was typical for all three dimensional models that contained

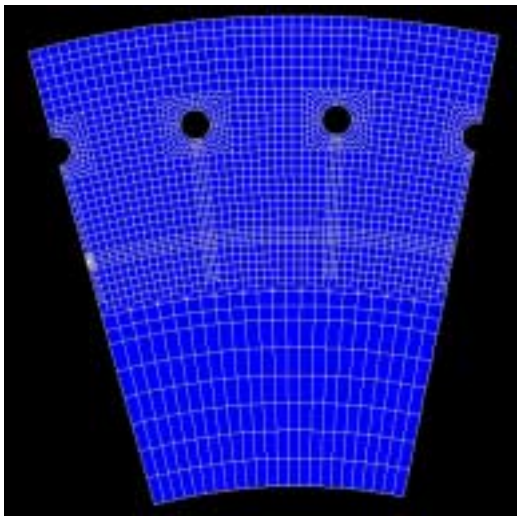

Fig. 3 A typical 2D FE model for the disc

semi-circular cracks or corner (quarter-circular) cracks

NISA II as well as MSC.Patran and MSC.Nastran FE packages were used to perform the calculations.

The direct displacement field approxi-mation method was used to extract the stress intensity factor from the finite element calculation results [6].

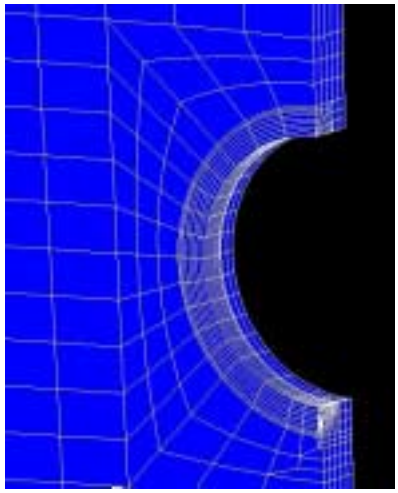

Fig. 4 A typical 3D FE model for the disc

3. RESULTS AND DISCUSSION

3.1 Finite Element Convergence Analysis

To find the effect of a disc segment sector angle on the stress distribution in the discs with cracks and also on the SIFs, a convergence analysis was performed using 2D FE models. In these calculations, cracks of the same length, 16.2 mm, were embedded in disc segments with sector angles varying in the range of 2.25° to 27.0°. The SIFs for thru-thickness cracks were obtained. A significant effect of the sector angle was found in the range of 0° to 18° on the *calculated* SIF. Therefore, 2D fracture mechanics calculations for one or two thru-thickness cracks emanating from the fracture critical points in disc bolt holes were performed using disc segments with a sector angle 27.0° or 29.25°. Three dimensional FE fracture mechanics calculations were performed using disc segments with much smaller sector angle, 4.5°, because very small cracks were analysed in these models and convergence was achieved for this sector size.

3.2 Stress Analysis

Fig. 5 presents typical von Mises stress distribution for the disc. A comparison of the 2D and 3D stress contours revealed good agreement. These results indicated that stress analysis in the relatively thin bolt holes area for

the compressor disc under a centrifugal load can be performed using a 2D FE modelling technique, instead of the more time consuming and cumbersome 3D modelling process.

Upon analysing the stress distribution in Fig. 5, it is noticeable that the hoop stress was the main contributing factor to the von Mises stress for two critical points in the bolt hole area. These critical points, denoted A and B in Fig. 2, are located at the intersections of the bolt hole circumference and a radial line drawn through the centre of the disc and the centre of the bolt hole. The hoop stress at Points A and B was of the order of 1023 MPa while von Mises stress was 1015 MPa. The stress at point C was mainly influenced by the radial stress component. Von Mises stress at this point was 319 MPa The von Mises stress in the bore area was 658 MPa. These bore stresses were considerably lower than the highest stresses in the bolt hole region.

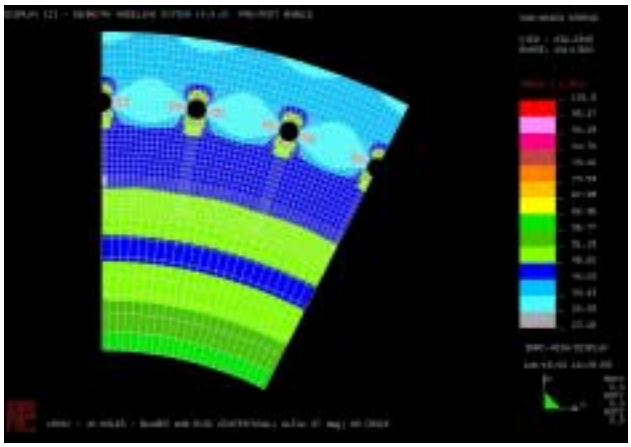

Fig. 5 Von Mises stress distribution (2D FE model)

The main conclusion, which can be drawn from the stress analysis results of the uncracked compressor discs, is that the fracture critical locations in terms of the magnitude of von Mises stresses, are points A and B (Fig. 2) located in the disc bolt hole area. This was in conformance with the cracking observed in service exposed discs [1-3]. The highest stresses in this area were approximately 75% of the lower bound of the yield strength value for AM355 steel. According to the results obtained, the LCF cracks are expected to initiate in the disc bolt hole region first. Therefore, in the subsequent fracture mechanics calculations all cracks in the disc were embedded in the bolt hole area.

3.3 Fracture Mechanics Analysis

As indicated earlier, to assure convergence fracture mechanics calculations on all 2D models were conducted using disc segments with sector angles of 27.0° or 29.25°, whereas for the 3D calculations disc segments with a 4.5° sector angle was used.

Fig. 6 illustrates the effect of the radially inward thru-thickness crack length on SIF for one crack, two cracks emanating from two bolt holes separated by one uncracked bolt hole and for two cracks in two neighbouring bolt holes.

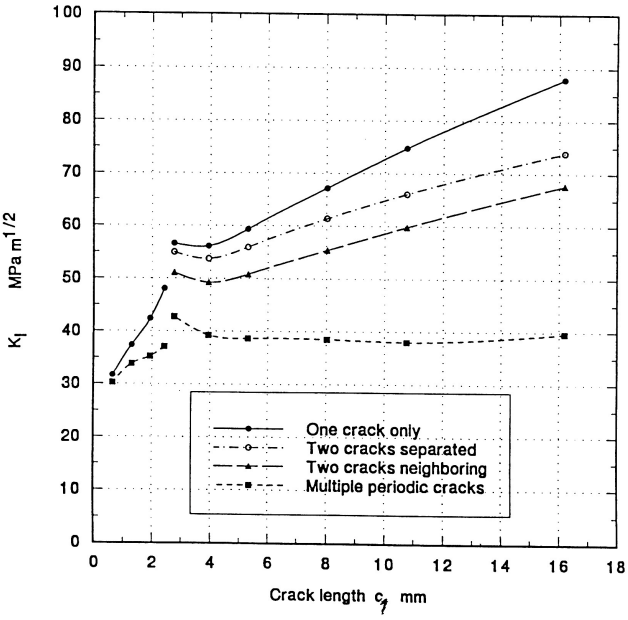

Fig. 6 SIF for through-thickness cracks emanating the bolt hole towards the disc centre (2D FE models)

The SIF for one or two radially inward thru-thickness cracks emanating from the bolt hole increased with an increase in crack length. In a disc containing only one crack, the SIF was estimated to be 32 MPam$^{1/2}$ for a crack length of 0.64 mm, which increased to a value of 57 MPam$^{1/2}$ for a c value of 2.8 mm and reached 88

MPam$^{1/2}$ when the crack length was 16 mm. If two radially inward cracks of equal length emanated from two bolt holes that were

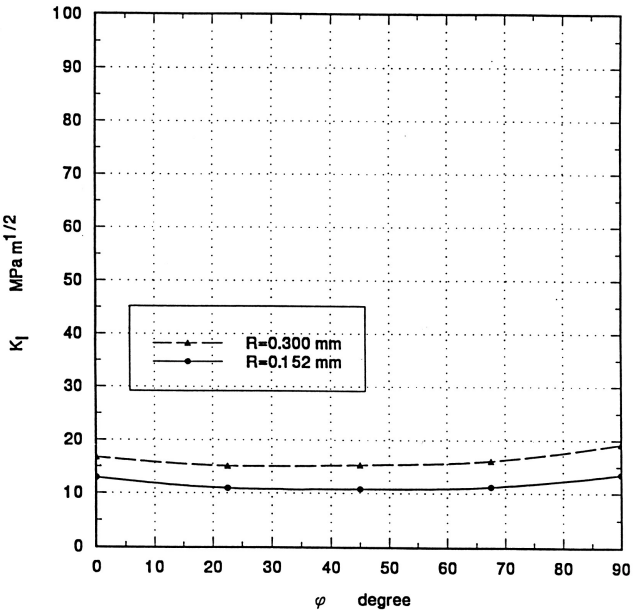

Fig. 7 SIF for corner cracks emanating from the bolt hole (3D models)

separated by one uncracked bolt hole the SIF values were lower. In this case the SIF was 55 MPam$^{1/2}$ for c=2.8 mm and increased to 74 MPam$^{1/2}$ for c=16 mm. If two radially inward cracks of equal length emanated from two neighbouring bolt holes, the SIF dropped even further in comparison with the two previous cases. The SIF was 51 MPam$^{1/2}$ for a crack length of 2.8 mm and 68 MPam$^{1/2}$ for a crack 16 mm in length. The SIFs were lowest when a crack was present in every bolt hole. These results are not totally unexpected because reduction in component stiffness as a result of component cracking reduces the disc stiffness and lowers the SIFs for a given crack length.

An important feature of results for the multiple bolt hole crack arrangement is that the SIF remains almost constant for crack lengths ranging between 4 and 16 mm.

Fig. 7 shows SIFs obtained from 3D FE calculations for corner cracks. The SIF were the lowest at the parametric angle of 45°, and the SIF gradually increased towards the surface of the bolt hole and towards the side surface of the disc.

The SIF curve for the corner crack R=0.15 mm was relatively flat, with the SIF at the crack tip (φ=45°) equal 11 MPam$^{1/2}$, which was only 2.5 MPam$^{1/2}$ smaller than the SIF at the intersection of the crack plane with the bolt hole and disc side surfaces (φ=0, φ=90°). The SIFs for the corner crack of radius R=0.30 mm were larger than those observed for a corner crack of radius R=0.15 mm. The SIF at the crack tip (φ=45°) of the corner crack was equal to 17 MPam$^{1/2}$ and it increased when the point of interest (described by φ) moved away from φ=45° towards φ=0 or φ=90° reaching approximately 19 MPam$^{1/2}$ at the free surfaces.

It was also found that the existence of a thru-thickness crack emanating from the bolt hole surface had a significant effect on the stresses in the opposite location of the hole (points A and B in Fig. 2). The stress in the uncracked location always increased with increasing through thickness crack size in the opposite location of the same bolt hole.

3.4 Quantitative Metallurgical Analysis

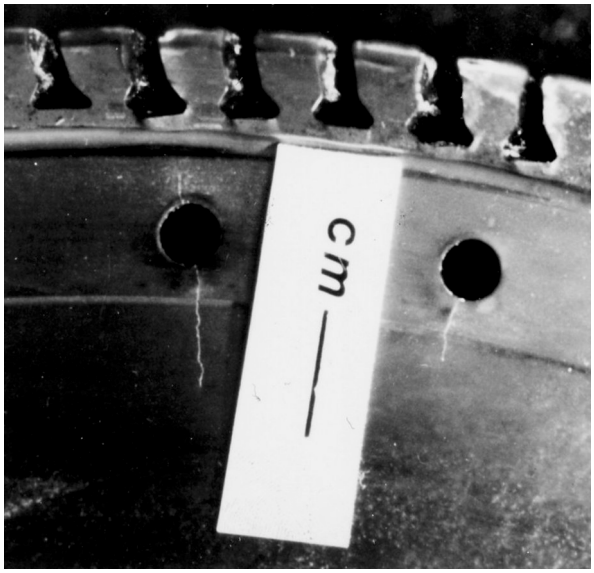

Fig. 8 Cracks emanating from bolt holes

Numerous service exposed discs containing natural cracks were available for metallurgical analysis, Fig. 8. To verify the SIF

calculation results for the compressor disc, a number of bolt hole regions were cut from a few cracked discs. To examine the fracture surfaces the cracks were pried open [3],[4].

Fatigue striation spacings were measured on the fracture surfaces of nine cracks ranging in length from 4 to 19 mm. The cyclic plastic zone radius (R_y) ahead of the crack tip was also measured for a number of bolt hole cracks to experimentally estimate the SIF range (ΔK) values. It is well known that during cyclic loading, a small zone of reversed plastic yielding called the cyclic plastic zone can be found, along with a larger monotonic plastic zone. The areas over which cyclic hardening or softening occurred as a result of plastic yielding was revealed by a series of microhardness measurements at the crack tip, where indentations were made at 0.05 mm space intervals at a load of 0.49 N.

Scanning electron microscopy (SEM) of the bolt hole cracks clearly established that a low cycle fatigue mechanism was responsible for initiating thumbnail cracks. Results indicated that most cracked bolt holes contained through-cracks with multiple crack initiation sites, Fig 8.

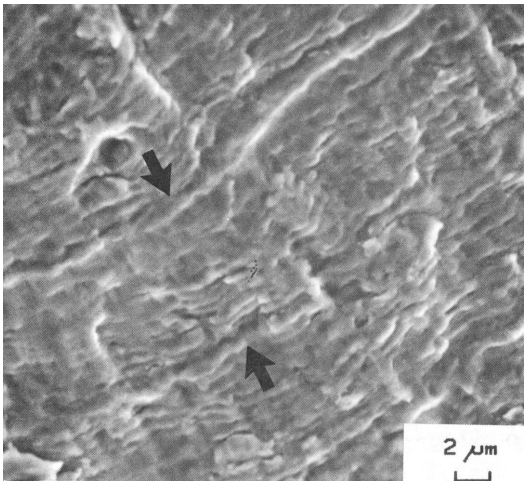

Fig. 9 Fracture morphology of bolt hole cracks [1], [2]

An important observation concerning the fracture surfaces was the formation of a banded or recurring striation pattern as indicated by arrows in Fig. 9. This recurring striation pattern consisted of discrete regions of finely spaced striations separated by a single, widely spaced

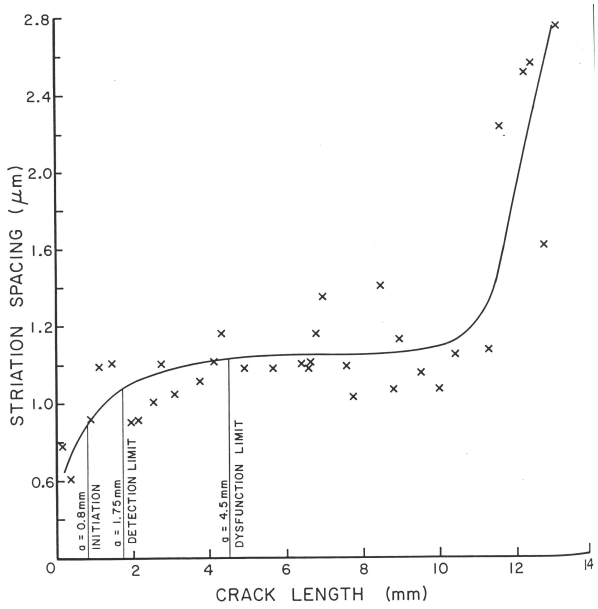

Fig. 10 Results of striation spacing measurements [1], [2]

striation. It is reasonable to assume that each discrete band represents the increment of crack growth that occurred during a single flight. Typical quantitative fractography results for a 14 mm long crack are shown in Fig. 10.

Average striation spacing for crack lengths less than 1 mm was 0.5 μm. For crack lengths between 1 and 10 mm the striation spacings were relatively constant at a value of approximately 1.1 μm. At crack lengths greater than approximately 10 mm the striation spacing increased sharply to about 2.5 μm. A constant striation spacing was indicative of a constant SIF up to a crack length of 10 mm. These results compared favorably with the results obtained on multiple bolt hole cracking results presented in Fig. 6.

In the compressor discs investigated, a large hardened zone was always located very close to the crack tip (Fig. 11). In a number of bolt hole specimens containing crack lengths ranging from 2 to 7 mm, the size of this hardened plastic zone did not vary significantly, indicating that ΔK was indeed constant and that *Ry* was approximately 0.45 mm. The *K* was

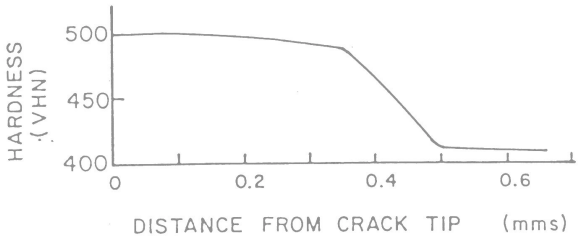

Fig. 11 Typical results of microhardness measurements at crack tip of compressor disc bolt hole cracks [1], [2]

calculated using the relation:

$$Ry = C\,(K/\sigma_y)^2$$

where σ_y is the yield strength and C is a constant that is dependent on material and type of loading. Assuming plane stress loading conditions because the discs are relatively thin, and using a value of $1/2\pi$ for C and 1100 MPa for σ_y the value of K was computed to be 58 MPa. This value is within the acceptable bounds of the FEM analysis results. Since approximately half of the bolt holes in some of the compressor discs had developed cracks during service, this result thus confirmed the accuracy of the FEM modeling techniques used to model multiple bolt hole cracking situation in this investigation.

4. CONCLUSIONS

It was established that the fracture critical location for the compressor disc was the bolt hole surface closest to the disc center, followed by a bolt hole surface closest to the disc rim. The LCF cracks were expected to initiate in these regions first, which was confirmed through field data obtained on life expired discs.

The largest values of SIFs were obtained for one radially inward, thru-thickness crack. This SIF is equal to 32 $MPam^{1/2}$ for a crack length of 0.64 mm and reached a value of 88 $MPam^{1/2}$ for a 16 mm crack. the crack.

The smallest values of SIF were obtained when multiple radially inward cracks emanated from every bolt hole. In this case the SIF remained almost constant, equal approximately to 40 $MPam^{1/2}$, for crack lengths ranging between 4 and 16 mm. The critical crack size for a simple thru-thickness crack emanating radially inwards from the bolt hole was of the order of 16 mm. The critical crack size was considerably longer for the multiple crack case. The FEM predicted SIF value was very similar to that predicted on the basis of striation spacing and plastic zone size measurements on actual service induced cracks.

The presence of an additional radially outward thru-thickness crack increased the SIF ahead of the crack tip of the radially inward thru-thickness crack emanating from the same bolt hole. For example, an additional outward crack 1.9 mm in length increases the SIF for radially inward cracks by approximately 3-7%.

Acknowledgement

This work was sponsored by the Canadian Department of National Defence

References

[1] Koul, A.K., Wallace, W., and Thamburaj, R. Problems and Possibilities for Life Extension in Gas Turbine Components, *Engine Cyclic Durability by Analysis and Testing, AGARD Conference Proceedings No. CP-368*, pp.10-1 - 10-32, 1984.

[2] Koul, A.K., Thamburaj, R., Raizenne, M.D., Wallace, W., DeMalherbe, M.C., Practical Experience with Damage Tolerance Based Life Extension of Turbine Engine Components, *Damage Tolerance Concepts for Critical Engine Components, AGARD Conference Proceedings No. CP-393*, pp. 23-1 - 23-22, 1985.

[3] Koul, A.K., Bellinger, N.C., and Fahr, A., Damage-Tolerance-Based Life Prediction of Aeroengine Compressor Discs: I. A Deterministic Fracture Mechanics Approach, *International Journal of Fatigue*, Vol. 12, No, 5, pp. 379-387.,1990.

[4] Koul, A.K., Bellinger, N.C., and Gould, G., Damage-Tolerance-Based Life Prediction of Aeroengine Compressor Discs: II. A Probabilistic Fracture Mechanics Approach, *International Journal of Fatigue*, Vol. 12, No, 5, pp. 388-396, 1990.

[5] *Aerospace Structural Metals Handbook, Volume 1*, CINDAS/Purdue University, 1992.

[6] Beres W., and Koul, A.K., Finite Element Calculation of Stress-Intensity Factors for Thumb-Nail Cracks in DEN Specimens, *Report of the Institute for Aerospace Research, National Research Council Canada, LTR-ST-1929*, 1993.